Hindawi
Advances in Civil Engineering
Volume 2021, Article ID 6612377, 13 pages
https://doi.org/10.1155/2021/6612377

Research Article

Degradation Behaviour of Deteriorated RC Beams Strengthened with CFRP under the Compound Effects of Acid-Salt Mist and Carbon Dioxide

Wei Wang,[1] Yuan-zhou Wu ,[2] and Zhongnian Fang[3]

[1]*School of Architectural Construction, Jiangsu Vocational Institute of Architectural Technology, Xuzhou 221116, China*
[2]*School of Mechanics and Civil Engineering, China University of Mining and Technology, Xuzhou 221116, China*
[3]*Institute of Architectural Design Research and Consulting Co., Ltd., China University of Mining and Technology, Xuzhou 221008, China*

Correspondence should be addressed to Yuan-zhou Wu; wyzcumt@126.com

Received 8 December 2020; Revised 14 April 2021; Accepted 13 May 2021; Published 26 May 2021

Academic Editor: Keerthan Poologanathan

The reinforcement effect and durability of carbon fibre-reinforced polymer (CFRP) sheets are important indicators that affect its promotion and application. This study conducted an experimental investigation of the degradation behavior of reinforced concrete (RC) beams strengthened with CFRP. The RC beams were deteriorated under the compound effects of acid-salt mist and carbon dioxide for a time period t_{1i}, then strengthened with one or two layers of CFRP sheets, and placed in the same deterioration environment for an additional time period t_{2i}. The failure modes, load-deflection curves, rigidity, and flexural carrying capacity changes were studied after the deteriorated RC beams were loaded to failure. Three combinations of deterioration periods were considered in this study: different t_{1i} and same t_{2i}, same t_{1i} and different t_{2i}, and same total time ($t_{1i} + t_{2i}$). This study found that the U-shaped hoops and the side concrete peeled off gradually as the CFRP-strengthened RC beams were deteriorated again with time. Under the ultimate load, the strengthening layer in the tension zone stripped. The strengthened layer, which consisted of CFRP, a binder, and the concrete cover, was stripped from the RC beam during loading. The deflection of the strengthened layer behaved differently from the other part; this disharmony prevented the mobilization of the tensile advantage of CFRP. The mechanism of RC beam's mechanical behaviour was analyzed in terms of the degrees of deterioration of RC beams and CFRP and their coupled effects. The conclusions of this study can be used as references in the prediction of strength changing and service life of strengthened RC beams.

1. Introduction

Reinforced concrete (RC) structures in coalmines deteriorate rapidly in their deteriorative environment. It is a common practice to strengthen RC structures to increase their reliability [1]. Fibre-reinforced polymers have been widely used to strengthen RC structures due to their lightweight, high tensile strength, good corrosion resistance, and easy construction [2]. In particular, the carbon fibre-reinforced polymer (CFRP) is widely accepted in RC structure-strengthening projects for its ability to increase the range of elastic area of RC structures, particularly when the tensile steel bars have yielded [3, 4].

Three failure modes can be observed when CFRP-strengthened RC beams are under their ultimate loads: the main failure mode is concrete crushed while the tensile steel bars are yielded and the CFRP strengthening layer is stripped [5]. As the RC beams deteriorate further, the other two failure modes can be observed: CFRP tensile fracture and bonding layer shear fracture [6, 7].

Epoxy glue, the organic binder to adhere CFRP onto concrete, has several shortcomings: (a) poor thermal stability and longer-term chemistry stability. The typical vitrification temperature (T_g) of the epoxy glue is 60–82°C. The elastic modulus and shear modulus of the epoxy glue decrease by approximately 90% when the temperature is 10°C

to 20°C out of the typical range of T_g [8]. (b) Greater flatness and smoothness of the concrete interface are required when grooves exist on the surface of concrete. The effective contact area between the concrete and binder decreases due to shrinkage of the epoxy glue. (c) Reverse tension is produced on the contact surface of the concrete, resulting in more ageing shrinkage on the interface of the CFRP and the stripped concrete [3, 9].

As confirmed above, strengthening with CFRP increases the mechanical performance of RC beams, although the performance degrades under environmental effects. The strengthening effect differs for RC beams with different degrees of deterioration. The degradation mechanism of CFRP-strengthened RC beam still needs further investigation. The deterioration mechanism relates to the deterioration of the RC beam and CFRP and particularly the coupling effect of the two, which remains unclear to researchers. Thus, this research conducted an experimental investigation of the degradation behavior of reinforced concrete (RC) beams strengthened with CFRP. The RC beams were deteriorated under the compound effects of acid-salt mist and carbon dioxide for a time period t_{1i}, then strengthened with one or two layers of CFRP sheets, and placed in the same deterioration environment for an additional time period t_{2i}. The failure modes, load-deflection curves, rigidity, and flexural carrying capacity changes were studied after the deteriorated RC beams were loaded to failure. Three combinations of deterioration periods were considered in this study: different t_{1i} and same t_{2i}, same t_{1i} and different t_{2i}, and same total time ($t_{1i} + t_{2i}$). The flexural failure modes, load-deflection curves, rigidity, and loading capacity of RC beams that deteriorated for 18 to 30 months in the compound effects of acid-salt mist and carbon dioxide then exposed in the same environment for another 15 to 21 months after being strengthened with CFRP are studied; therefore, the mechanical performance of the RC beams in the deteriorative environment before and after strengthening and factors that affect the performance are analyzed in this paper. The research results better reflect the actual situation of the damage and deterioration of colliery ground RC structures and provide effective guides to the strengthening of deteriorated RC structures.

2. Experimental Program

2.1. Materials and Beam Specimen. Ordinary 32.5-grade Portland cement with a specific gravity of 3.18 and a specific surface area of 350 m^2/kg was used in this investigation. The coarse aggregate was crushed stone with a maximum size of 16 mm. Natural river sand, medium size with a fineness modulus of 2.42, was used as the fine aggregate in this study. The ratio of fine aggregate to coarse aggregate was a fixed number of 35%. Concrete mixtures were designed according to the Chinese Standard JGJ55 [10] and GB50367 [11]. The mixture's weight proportion was water: cement: fine aggregate: coarse aggregate = 192 : 343 : 576 : 1063, with a 28-day cubic compressive strength of 35.2 MPa. The properties of the CFRP and binder used in the experiment are shown in Table 1.

The beam specimens had a length of 1,500 mm and a rectangular cross section of 100 mm × 200 mm (width × depth). The dimensions of the beam specimens are shown in Figure 1(a). Two plain round bars with diameters of 8 mm were placed at the top of the beam as hangers, and two 12 mm diameter ribbed bars were placed at the bottom of the beam as tensile rebar. The concrete cover was 15 mm thick. The yield and ultimate rebar strengths were 380 and 552 MPa, respectively. After a designed period of deterioration, the RC beams were strengthened with CFRP, as shown in Figure 1(b). Two layers of CFRP with the same width of the beam were adhered on the bottom of the RC beam, and three U-shaped hoops with a width of 50 mm were adhered to the sides and bottom of the beam in the shear section on each ends of the beam. The first hoop to the end of the beam was placed at 150 mm from the end. The spacing between each of the four hoops was 100 mm. To keep the reinforcing effect, two CFRP sheets with the width of 5 cm are used to strengthen both sides of the compression zone.

2.2. Test Design. Twelve beam specimens, designated as L0 through L11, were made for this study. L0 and L1 were the control specimens, and L2 through L11 were placed in a simulated deteriorative environment. In the simulated environment, salt mist consisting of NaCl, $MgCl_2$, and Na_2SO_4 was sprayed on the beam specimens. Alternating spraying, drying, and freeze-thaw cycles were applied. The spray contents and simulation environment are listed in Table 2.

As shown in Table 3, the eleven specimens, L1 through L11, were first placed in the simulation environment for a period of t_{1i} and then strengthened with CFRP. The strengthened specimens were placed back to the same environment for a second period of t_{2i}, where i stands for the specimen Li. Based on the research results of [1, 12], the investigation time was determined with 3 months per cycle. Three combinations of deterioration periods were considered in this study: (a) $t_{1i} = 18$ to 30 months and $t_{2i} = 15$ months; (b) $t_{1i} = 21$ months and $t_{2i} = 15$ to 21 months; (c) $t_{1i} + t_{2i} = 42$ months. All eleven test specimens were cast by the same batch. To accelerate deterioration, sodium chloride with 10% of water weight was added to beams L2, L4, and L7 during concrete mixing. After curing for 28 days and then sitting in the regular laboratory room condition for 7 months, the beam specimens were placed in the simulation environment. The deterioration conditions of the beam specimens were examined every three months.

After the two deterioration periods, the test beams were ready to be tested. As shown in Figure 2, the specimens were simply supported and subjected to the four-point bending test. Each specimen had a clear span of 1,200 mm and shear spans of 400 mm. Bending was constant in the central zone with a length of 400 mm. A hydraulic jack was used to apply the static load through a steel spreader beam. Transducers were used to collect the displacement data at the midspan, loading points, and supports. A schematic of the transducer arrangement is shown in Figure 2.

Table 1: Properties of CFRP and binder used in the experimental test.

Material	Thickness (mm)	Tensile strength (MPa)	Elastic modulus (MPa)	Elongation (%)	Compressive strength (MPa)	Flexural strength (MPa)	Shear strength (MPa)
CFRP	0.111	32.35×10^2	2.160×10^5	1.5	—	—	—
Binder	—	57.94	2.804×10^3	—	86.03	76.20	26.96

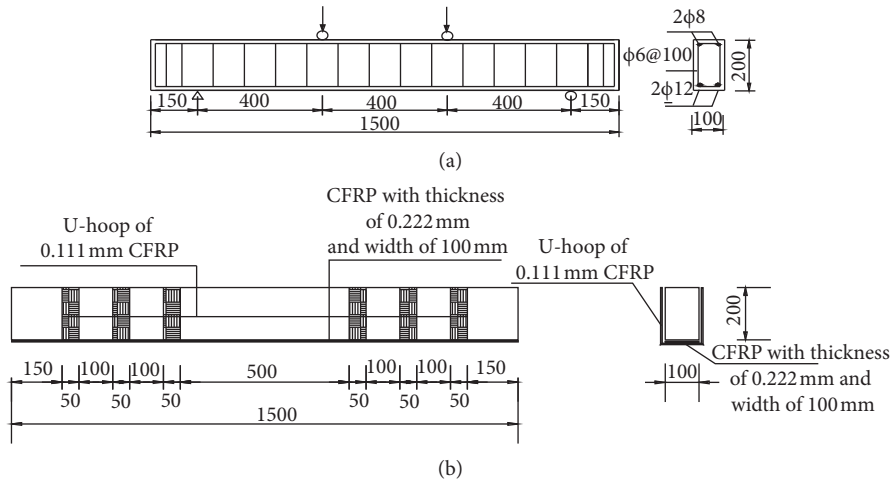

Figure 1: Configuration of test specimens and strengthening method (unit: mm). (a) Configuration of the test specimen (unit: mm). (b) RC beam strengthened with CFRP.

Table 2: Design of the simulation environment.

NaCl (mass ratio) (%)	$MgCl_2$ (Mass ratio) (%)	Na_2SO_4 (Mass ratio) (%)	CO_2 (mg/m^3)	HCl (mg/m^3)	Temperature (°C)	Humidity (%)
0.25	2.71	10	5778	128	50	75

Table 3: Parameters of the experimental beams.

No.	Length × width × depth (mm)	t_{1i} (months)	t_{2i} (months)	Remarks
L0	$1500 \times 100 \times 200$	0	0	
L1		0	0	
L2		18	15	
L3		18	15	Sodium chloride with 10% of water weight added
L4		21	15	
L5		21	15	Sodium chloride with 10% of water weight added
L6		21	18	
L7		24	15	
L8		21	21	Sodium chloride with 10% of water weight added
L9		24	18	
L10		27	15	
L11		30	15	

After the bending test, concrete cores were drilled from the ends of the beams and the corroded rebars were obtained from the specimens. A 1% phenolphthalein alcohol solution was sprayed on the surface of the core as a pH neutralization indicator. The maximum and minimum pH neutralization depths as well as various median values were recorded, and the average value was taken as the neutralization depth. The concrete cores were axially loaded to obtain their compressive strengths. The rebars were loaded for tensile strengths after the corrosive ratios were checked.

3. Results and Discussion

3.1. Deterioration and Failure Mode Characteristics. Cracks appeared on the top of the beams along the hanger bars, except in beams L10 and L11. The U-shaped hoops of strengthened beams L6, L8, and L9 peeled off when they were re-deteriorated for more than 18 months. Cracks also appeared on the sides of the RC beams along the direction of the tensile steel bars, with the maximum crack width exceeding 6 mm. The reinforcement layer, including the

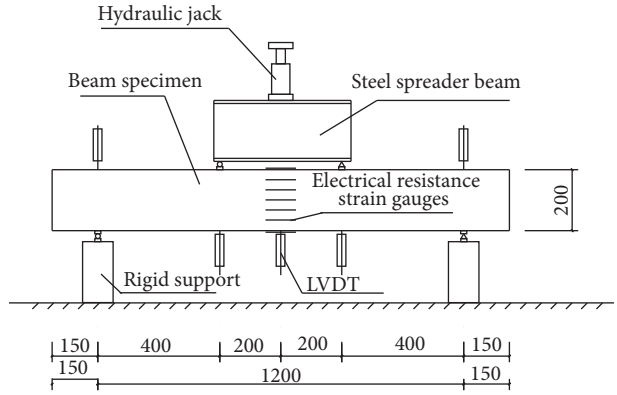

Figure 2: Schematic of experimental setup and instrumentation (unit: mm).

concrete cover, noticeably stripped from the RC beam but did not peel off with the effect of the U-shaped hoop.

The deterioration characteristics of the RC beams and flexural loads are presented in Table 4, where f_{cu} is the concrete strength after the test, $X(t)$ is the neutralization depth, η is the rebar mass loss ratio, η is the weight loss ratio of the rebar, F_u is the ultimate flexural load, Δ_y and Δ_u are the midspan deflection of the beam specimens under the yield and ultimate flexural load, respectively, and μ_Δ is the ductility of RC beams.

Figure 3 illustrates the deterioration before the test and failure modes of the test beam specimens after the test.

Under the ultimate load, all RC beams except beam L8 failed with the reinforcement layers peeling off together with the concrete cover. In the loading process, a noticeable sound was noticed when the CFRP wires pulled off, and the reinforcement layers broke suddenly as brittle failure occurred. The U-shaped hoops of beam L8 peeled off when the concrete was compressed; thus, the compressive area decreased heavily, and the concrete was compressively crushed.

3.2. Carrying Capacity. The ultimate carrying capacity of the test beams is illustrated in Figure 4.

Except for L2, L7, L10, and L11, the carrying capacity of the re-deteriorated beams decreased considerably compared with that of beams L0 and L1, with a maximum reduction of 46%. As the protective covers of beams L10 and L11 were recasted before strengthening, their carrying capacities increased to close to or higher than those of beams L0, L1, and L2 and other beams. Several trends were observed. (a) With the increase of the deterioration time *ti1*, the carrying capacity of the strengthened beam decreased with the same redeterioration time ti2, the carrying strength of beam L4, L5, and L6 was less than that of beam L2 due to the effect of different former deterioration time ti1. (b) If the total deterioration time $ti1 + ti2$ was the same, the capacity of the strengthened beam decreased as the time $ti1$ increased, such as beams L6 and L7. The same phenomenon was observed in beams L10 and L11. (c) The sodium chloride introduced in the concrete mix speeded up the deterioration process which was observed by comparing L8 with other beams.

3.3. Load-Deflection Curves. The load-deflection curves of test beams are shown in Figure 5.

As shown in Figure 5, the inflection points corresponding to the cracking loads cannot be determined on the load-deflection curves of the re-deteriorated beams. When the beams yielded, they maintained large rigidities till brittle failure. This is mainly due to the mechanical character of CFRP, not to that of the steel bar. The elastic modulus of CFRP is greater than that of the steel bar, and thus, the strain of CFRP is smaller than that of the steel bar under the same load. The brittleness of the reinforcement layer was greatly enhanced as two layers of CFRP were attached to it. When the load reached the ultimate value, brittle fracture of CFRP occurred and the beam failed with minor noticeable deformation. The yield platform was relatively noticeable for the deteriorated beams because those beams were seriously deteriorated and entered the yield stage prematurely.

3.4. Concrete Strain in the Midspan. Strain gauges were set up on the side and bottom of the test beams to collect the strain data during the static loading test. The collected data are shown in Figure 6.

Before the beam yielded, the concrete strain in the midspan of the RC beams increased linearly with the distance from the centre axis, which indicated that the plane section assumption was suitable for the carrying capacity calculation of the strengthened beams. As the load increased, particularly when the load exceeded the yielding load, the tensile strain increased continuously, whereas the compressive strain remained relatively constant until the beams failed. This is due to the cracks caused by the corrosion of the hanger steel bars, which led the concrete in the compression zone to be gradually peeled off with load increasing. As the strain gauges were destroyed by the cracks, the measured value corresponding to the ultimate load decreased to zero, as shown in Figures 6(c) and 6(e).

3.5. Tensile Strain of CFRP. Five resistance strain gauges with a length of 50 mm were longitudinally attached to the pure bent section of the test beams to record the CFRP strain. The test results are shown in Figure 7.

Table 4: Basic parameters of deteriorated RC beams.

No.	Time (months)	f_{cu} (MPa)	$x(t)$ (mm)	η (%)	F_u (kN)	Δy (mm)	Δu (mm)	μ_Δ	Failure mode
L0	0	35.2	0	0	80	3.05	10.21	3.35	CC
L1	0	35.0	0	0	78	2.98	10.39	3.49	CC
L2	18 + 15	25.9	24.5	11.64	89	3.11	11.73	3.77	PS
L3	18 + 15	24.3	24.9	14.33	70	3.80	8.66	2.28	PS
L4	21 + 15	23.8	25.4	15.46	75	4.93	9.77	1.98	PS
L5	21 + 15	17.4	28.8	14.35	68	3.14	8.38	2.67	PS
L6	21 + 18	15.8	31.4	19.11	65	4.42	13.35	3.02	PS
L7	24 + 15	20.4	30.4	19.36	84	4.74	11.46	2.42	PS
L8	21 + 21	25.84	—	23.26	43	4.15	9.82	2.37	CC
L9	24 + 18	22.09	—	19.30	55	4.47	9.96	2.23	PS
L10	27 + 15	22.26	—	21.17	85	3.98	11.43	2.87	PS
L11	30 + 15	20.48	—	22.75	90	4.48	11.03	2.46	PS

Note: (a) time "18 + 15" means that $t_{1i} = 18$, and $t_{2i} = 15$, and the same as follows. (b) CC = crushing of concrete in the compression zone; PS = peel off of CFRP. (c) As the concrete cover of the beam L10 and L11 were lost, the grouting material was used to re-cast the protective layer firstly, and then, the beams were strengthened with CFRP like the others.

At the initial loading stage, the strain of CFRP increased with the load increasing, and the values were relatively similar at each measuring locations. When the beam cracked, the strain increased dramatically. This increase became particularly large when the beam entered the yielding state. Under the ultimate load, large gaps appeared between the CFRP strains at different locations and the maximum strain value was not necessarily in the middle of the beam. The beams strengthened with CFRP had good durability to the compound effects of acid-salt mist and carbon dioxide. Due to the serious deterioration of the RC beam, concrete at some locations cracked and peeled off during the loading process. The CFRP strains at these locations were inconsistent with those at the other locations, resulting in local stress concentration and large strains. The CFRP strengthening layer, consisted of CFRP, a binder, and the concrete cover, was too brittle to bear the flexural load; therefore, the tensile strain of CFRP was not effectively utilized.

4. Experimental Analysis

Five failure modes of the RC beams strengthened with CFRP under the ultimate load have been reported in various literatures [12–14]. The five failure modes are as follows. (I) Concrete in the compression zone was crushed, while the tensile steel bars did not reach their yielding strengths, and the strain of CFRP did not reach its ultimate value. (II) Concrete in the compression zone was crushed, and the tensile steel bars reached their yield strengths, and the strain of CFRP did not reach its ultimate value. (III) The tensile steel bars yielded, and the strain of CFRP reached its ultimate value, while the concrete in the compression zone was not crushed. (IV) The strengthening layer, which consisted of a concrete protective cover, a binder, and CFRP, was sheared to peel off. (V) CFRP separated from the concrete cover of the RC beam. Failure modes (I) and (IV) occurred in this study.

As failure mode (I) occurred, several assumptions are adopted to calculate the carrying capacity of the strengthened RC beams. (a) All of the assumptions used in the calculation model of the RC beam strengthened with CFRP illustrated in the Chinese standard of Code for Design of Strengthening Concrete Structures GB50367 are satisfied. (b) The strain of CFRP ε_{cf} satisfies the plane section assumption, and the value of ε_{cf} is less than the design value $[\varepsilon_{cf}]$. (c) Failure (IV) did not occur in the RC beam under the ultimate load. The calculation model of the RC beam strengthened with CFRP corresponding to failure mode (I) is shown in Figure 8.

The height of compressive zone x is less than the ultimate value x_{cr}, and the strain of tensile steel bar ε_s is less than the yield value ε_y; it is taken that $\varepsilon_s = \varepsilon_y$. The concrete strain ε_c exceeds the ultimate value ε_{cu}, and then, $\varepsilon_c = \varepsilon_{cu}$. The tensile strain of CFRP ε_{cf} is less than the design value $[\varepsilon_{cf}]$, which is equal to two thirds of the ultimate strain of CFRP, which has a value of 0.01. Then, according to the assumptions, $\varepsilon_{cf} = [\varepsilon_{cf}]$, and the flexural carrying capacity of the strengthened RC beam can be calculated as follows:

$$M_u = f_y A_s \left(h_0' - \frac{x}{2}\right) + E_{cf}\varepsilon_{cf}A_{cf}\left(h' + \frac{A_{cf}}{b'} - \frac{x}{2}\right), \quad (1)$$

$$\alpha_1 E_c \varepsilon_c b' x = f_y A_s + \varphi_{cf} E_{cf}[\varepsilon_{cf}] A_{cf} - f_{yc}' A_s', \quad (2)$$

$$\varphi_{cf} = \frac{0.8\varepsilon_{cu}h'/x - \varepsilon_{cu} - \varepsilon_{cf0}}{\varepsilon_{cf}}, \quad (3)$$

and x_{cr} can be obtained by the following equation:

$$x_{cr} = \frac{x_b}{h} = \frac{\beta_1 \varepsilon_{cu}}{\varepsilon_{cu} + [\varepsilon_{cf}]}, \quad (4)$$

where M_u is the ultimate bending moment of the strengthened RC beam, A_s is the cross-section area of the tensile steel bar, h_0' is the effective cross-section height of the deteriorated RC beam, h' is the cross-section height of the deteriorated RC beam strengthened with CFRP, b' is the effective cross-section width of the deteriorated RC beam, E_{cf} is the elastic modulus of CFRP, A_{cf} is the sectional area of CFRP, φ_{cf} is the effective utilization rate of CFRP, f_{yc}' and f_y' are the yield strength of the compressive and tensile steel bar, respectively, A_s' is the cross-section area of the compressive

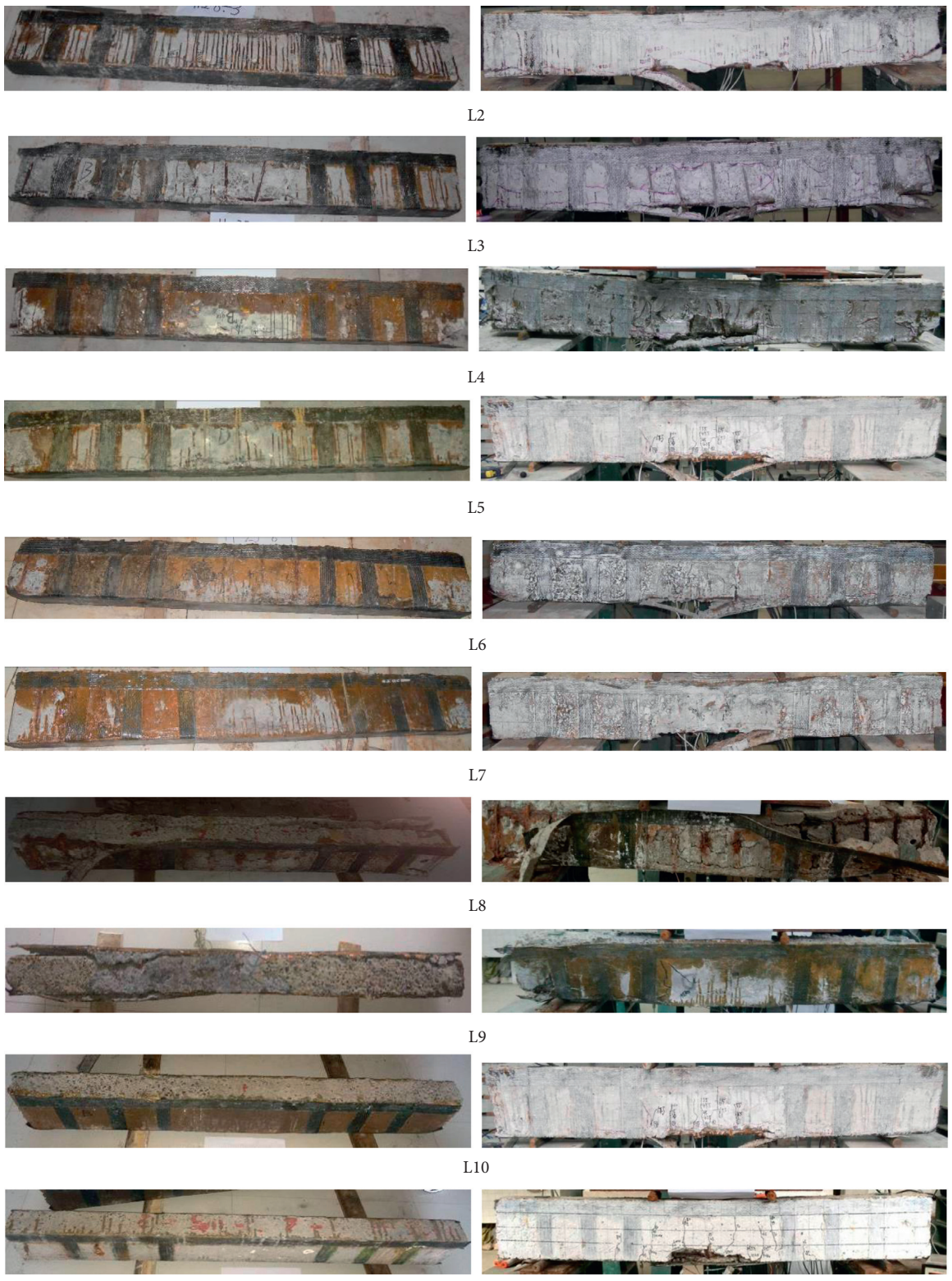

Figure 3: Deterioration and failure modes of beams.

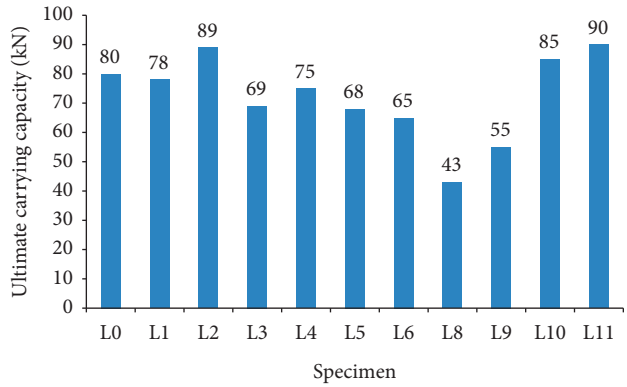

Figure 4: Ultimate carrying capacity of test beams.

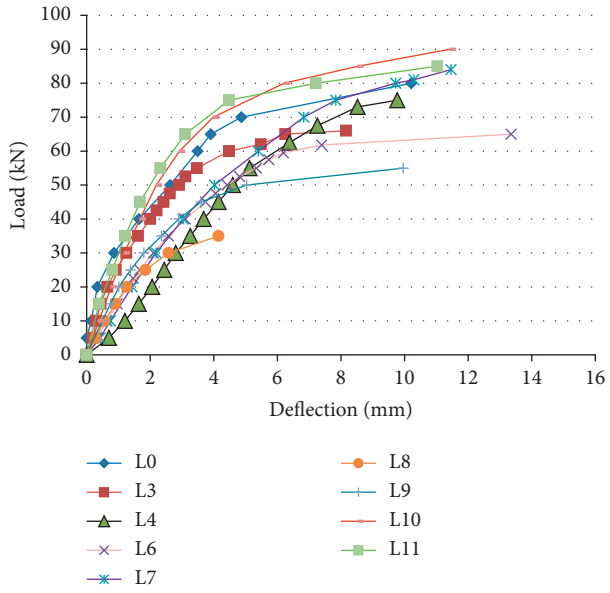

Figure 5: Load-deflection curves of test beam specimens in the midspan.

steel bar, ε_{cf0} is the lagged strain of CFRP, and α_1 and β_1 can be obtained from the Chinese standard GB50367.

As failure mode (IV) occurred, the CFRP was sheared off and the RC beam failed immediately. The strain of concrete in compression zone $\varepsilon c \leq \varepsilon cu$, and the steel bar tensile strain $\varepsilon s \geq \varepsilon y$, whereas the CFRP tensile strain examined that εcf was less than the ultimate value of $[\varepsilon cf]$. CFRP shear failure typically occurred on the side of the U-shaped hoop close to the pure flexural zone. The carrying capacity of the strengthened RC beam can be calculated by the following formula:

$$G_c \tau b' h' + G_{cf} \tau_{cf} A_{cf} + f'_v A'_s + f_v A_s = F_S, \quad (5)$$

where G_c and G_{cf} are the shear modulus of concrete and the CFRP strengthening layer, respectively, τ and τ_{cf} are the shear strain of concrete and the CFRP strengthening layer, respectively, f_v and f'_v are the shear capacity of the tensile and compressive steel bar, respectively, and F_S is the shear bearing capacity of the strengthened RC beam.

Based on equations (1) and (5), the carrying capacity of the strengthened RC beam is affected by the deterioration of the RC beam and the CFRP strengthening layer. Thus, the mechanism should be analyzed according to these two factors.

4.1. Deterioration of RC Beams. The following have been observed as the RC beam deteriorated [12]:(a) the compressive strength of the deteriorated concrete decreased; (b) the local sectional geometry of the RC beam decreased as the steel bars corroded, leading to the cracked and peeling of the concrete; (c) the cross-sectional area of the corroded steel bars decreased, and the tensile strength decreased; and, (d) the bond performance between the deteriorated concrete and corroded steel bars degenerated.

As the concrete deteriorated, the compressive strength decreased and the failure mode of the RC beam changed. With the decrease of the concrete tensile strength, the confining force to the steel bars decreased. Furthermore, as the steel bar corroded and expanded, the bonding concrete on the steel bar was under radical compression. The width of microcracks in the concrete was widened, and the concrete cover cracked [13–16]. In the corrosive environment, the concrete deterioration and steel bar corrosion occurred at the same time and affected each other [12, 17]. Tepfer [18] stated that the concrete around the steel bar should be divided into two parts:(a) a cracked inner part with an external diameter R_i and an internal diameter R_0, where R_0 is the initial diameter of the deformed steel bar; and, (b) an elastic outer part with an external diameter R_c and internal diameter R_i. Furthermore, $R_c + R_0 = c$. As the concrete compressive strength reduction was coupled with the steel bar corrosion, R_0 increased, while R_c decreased to zero. Then, the bond between the concrete and steel bar decreased to a nonbond. As a result, the effective sectional height and rigidity of the RC beam decreased.

4.2. Deterioration of the CFRP Strengthening Layer. Due to the poor infiltration of the epoxy resin to concrete, the CFRP, epoxy resin, and concrete surface layer produced a thin reinforcement layer. In the corrosive environment, the epoxy resin aged and changed the strengthening layer into a brittle sheet. Under the effect of moisture and temperature, the strengthening layer was stripped with the concrete of the RC beam [19–21]. Figure 9 illustrates the deflections of the strengthening layer and the steel bar under the ultimate load.

Ideally, the deflection of the strengthening layer should be equal to that of the steel bar, i.e., $\delta_1 = \delta_2$ and $\theta_1 = \theta_2 = \theta_3 = \theta_4$. As the strengthening layer became brittle, the actual state was $\delta_1 > \delta_2$, $\theta_1 > \theta_3$, $\theta_2 > \theta_4$, and $\theta_1 \neq \theta_2$. Then, shear force was produced due to the difference between the deflections of the strengthening layer and steel bar. Under the constraint of the U-shaped hoop, the deflections of the strengthening layer and steel bar were the same in the position of the U-shaped hoop. Thus, reverse shear force was produced. Therefore, shear failure occurred under the interaction between the two shear forces, and the normal tensile properties of CFRP were not utilized.

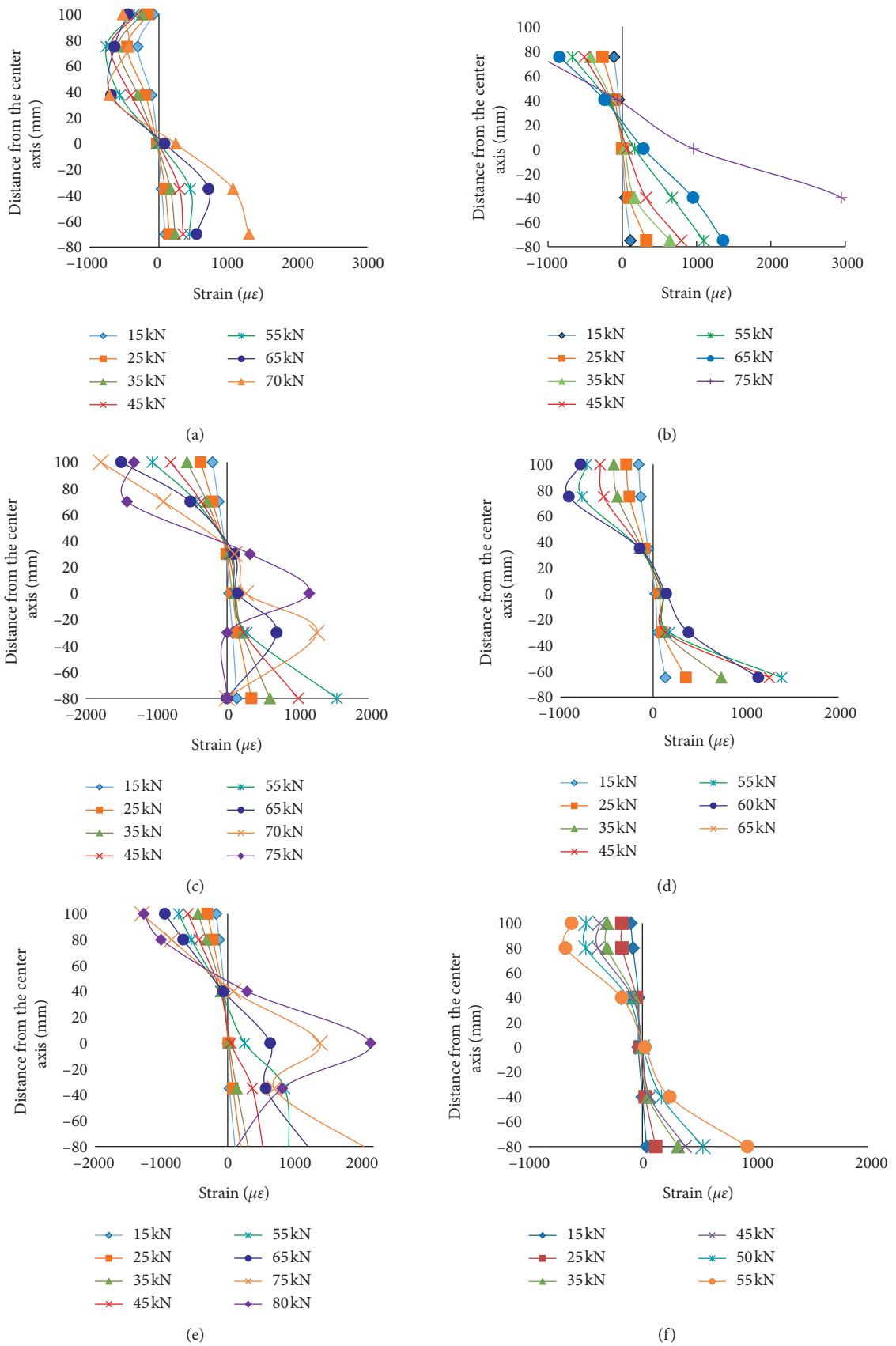

Figure 6: Continued.

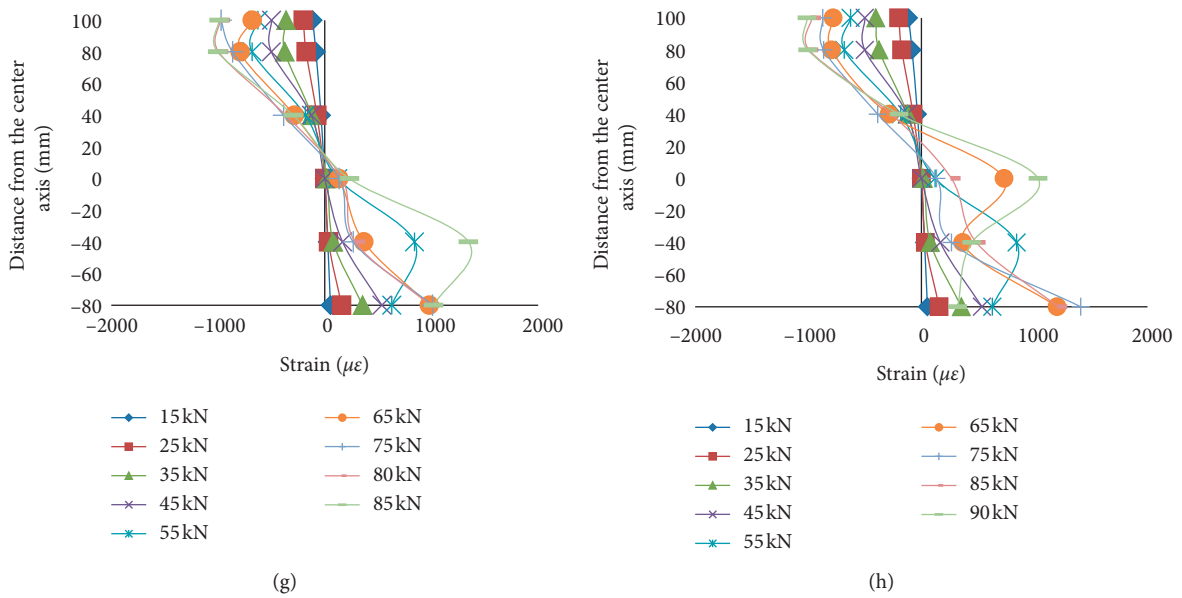

(g) (h)

Figure 6: Cross-sectional strain distribution of the test beams. (a) Beam L3. (b) Beam L4. (c) Beam L5. (d) Beam L6. (e) Beam L7. (f) Beam L9. (g) Beam L10. (h) Beam L11.

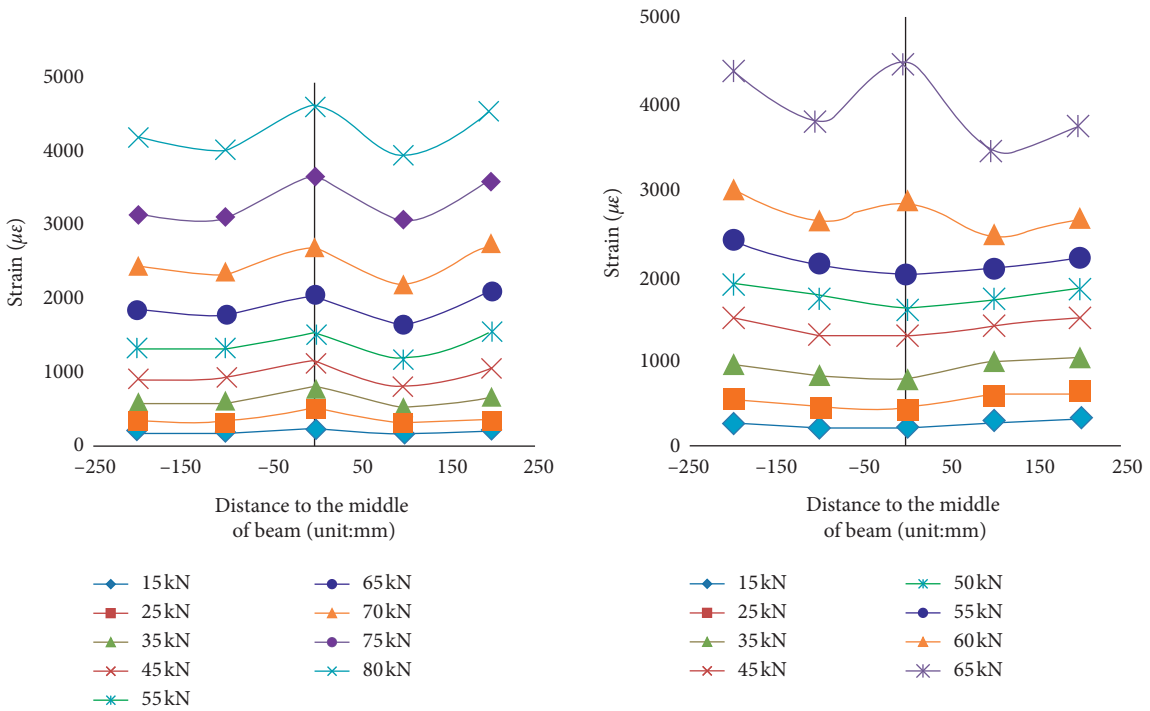

(a) (b)

Figure 7: Continued.

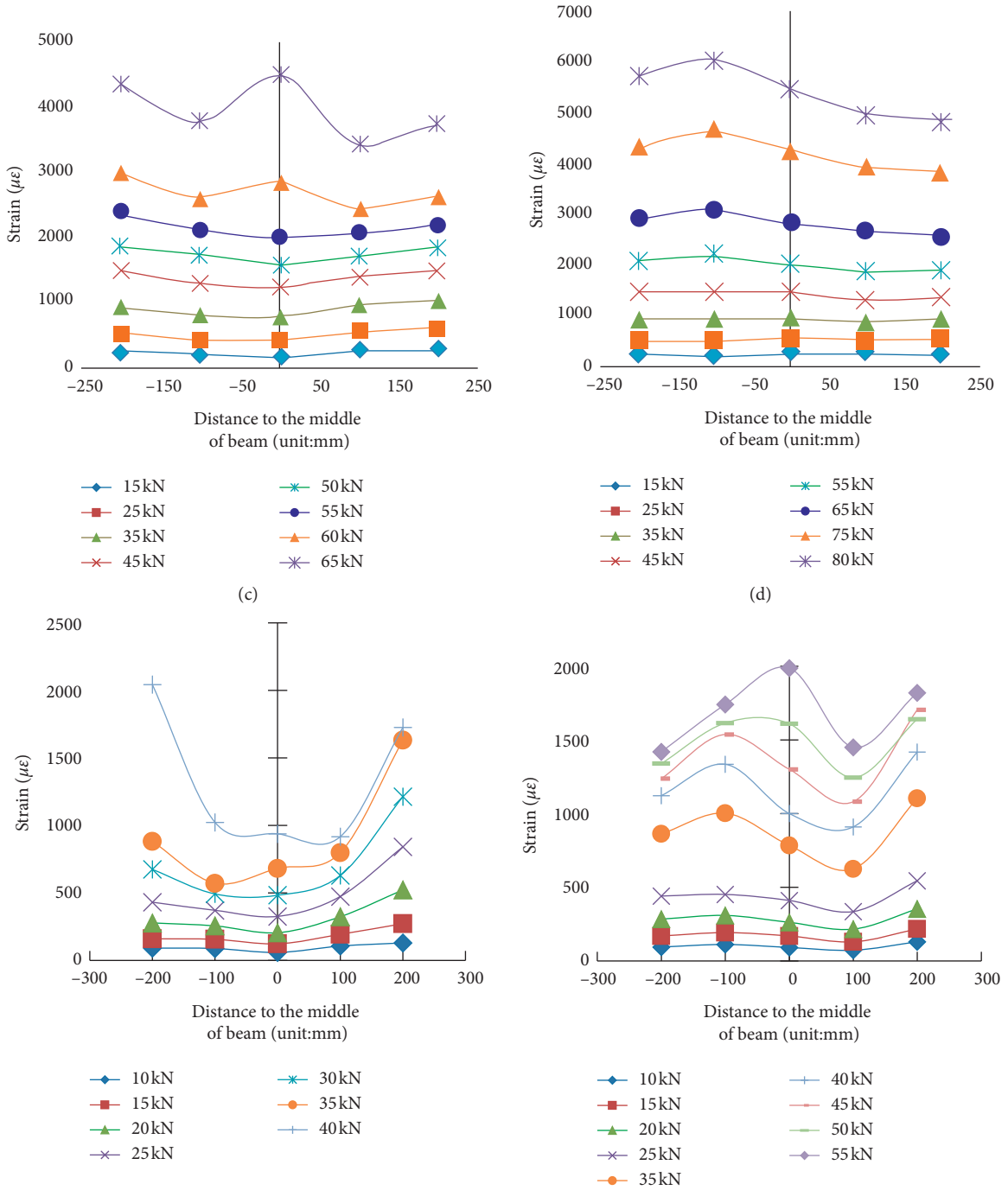

Figure 7: Continued.

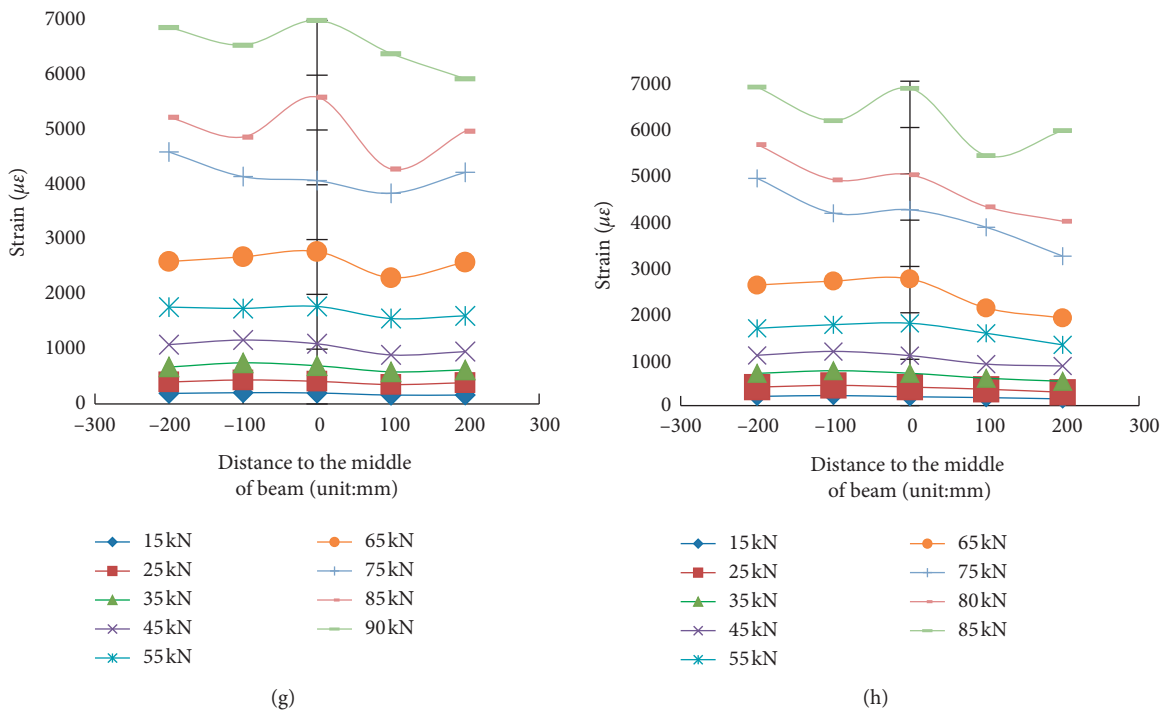

Figure 7: Strain of CFRP in the pure bending section of RC beams. (a) L3. (b) L5. (c) L6. (d) L7. (e) L8. (f) L9. (g) L10. (h) L11.

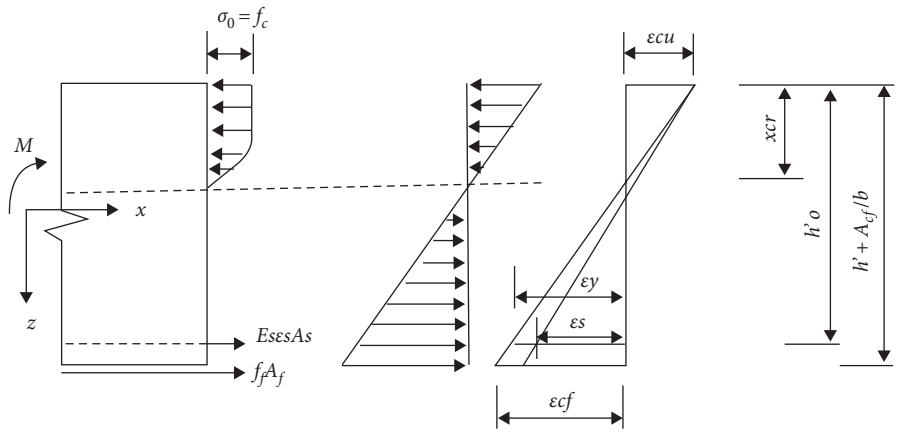

Figure 8: Calculation model of the RC beam strengthened with CFRP corresponding to failure mode I.

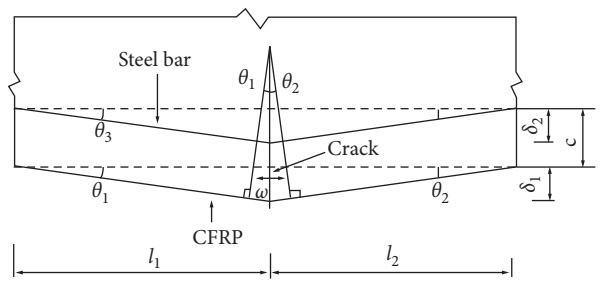

Figure 9: Crack of the strengthened beam under loading.

As the deterioration time increased, the RC beam and CFRP were further deteriorated, and the bond between them decreased continually. The displacement ductility coefficient of the strengthened beam became smaller as the RC beam deteriorated heavier during the time ti1.

5. Conclusions

(a) Under the joint effects of acid-salt mist and carbon dioxide, the deteriorated RC beam strengthened with CFRP was deteriorated again. Surface concrete was peeled off by tensile force generated by the U-shaped hoops. Stripping failure occurred in the strengthened layer in the tensile zone under the ultimate load.

(b) As the deterioration time increased, the carrying capacity of the re-deteriorated beams decreased considerably compared with that of beams L0 and L1, with a maximum reduction of 46%. With the increase of the deterioration time t_{i1}, the carrying capacity of the strengthened beam decreased even though they had the same strengthening mode and re-deterioration time t_{i2}.With the same deterioration time t_{i1}, as the re-deterioration time t_{i2} increased, the carrying capacity of the beam decreased considerably with a value of 33–43%. If the total deterioration time $t_{i1} + t_{i2}$ was the same, the capacity of the strengthened beam decreased as the time t_{i1} increased.

(c) The plane section assumption was satisfied for the carrying capacity in the investigation of the beam specimens until they yielded.

(d) The strengthened layer, which consisted of CFRP, a binder, and the concrete cover, was stripped from the RC beam during loading. The deflection of the strengthened layer behaved differently from the other part, and this disharmony prevented the mobilization of the tensile advantage of CFRP.

(e) The conclusions of this study can be used as references in the prediction of strength changing and service life of strengthened RC beams.

Data Availability

The data used to support the findings of the study are included with the article.

Conflicts of Interest

The authors declare that they have no conflicts of interest.

Acknowledgments

The investigation was supported by Science and Technology Project of Construction System in Jiangsu Province (Contract number: 2018ZD106), Key University Science Research Project of Jiangsu Province (Contract number: 20KJA560002), and "Xuzhou Science and Technology Project" (Contract no. KC16SS088).

References

[1] H.-L. Lv, Y.-Z. Wu, Z.-N. Fang, and S.-C. Zhou, "Deterioration behavior of reinforced concrete beam under compound effects of acid-salt mist and carbon dioxide," *Construction and Building Materials*, vol. 77, no. 77, pp. 253–259, 2015.

[2] U. Ebead and H. Saeed, "Flexural and interfacial behavior of externally bonded/mechanically fastened fiber-reinforced polymer strengthened reinforced concrete beams," *ACI Structural Journal*, vol. 111, no. 4, pp. 741–752, 2014.

[3] G. El-Saikaly and O. Chaallal, "Extending the fatigue life of reinforced concrete T-beams strengthened in shear with externally bonded FRP: upgrading versus repairing," *Journal of Composites for Construction*, vol. 19, no. 1, Article ID 04014027, 2014.

[4] J. Thamboo, S. Navaratnam, K. Poologanathan et al., "Characteristics of CFRP strengthened masonry wallettes under concentric and eccentric compression," *Case Studies in Construction Materials*, vol. 14, Article ID e00472, 2020.

[5] W. Xue, Y. Tan, and L. Zeng, "Flexural response predictions of reinforced concrete beams strengthened with prestressed CFRP plates," *Composite Structures*, vol. 92, no. 3, pp. 612–622, 2010.

[6] S. Hong, "Effects of the amount and shape of carbon fiber-reinforced polymer strengthening elements on the ductile behavior of reinforced concrete beams," *Mechanics of Composite Materials*, vol. 50, no. 4, pp. 427–436, 2014.

[7] E. R. K. Chandrathilaka, J. Gamage, and S. Fawzia, "Mechanical characterization of CFRP/steel bond cured and tested at elevated temperature," *Composite Structures*, vol. 207, pp. 471–477, 2019.

[8] T. T. D. Nguyen, K. Matsumoto, Y. Sato, A. Iwasaki, T. Tsutsumi, and J. Niwa, "Effects of externally bonded CFRP sheets on flexural strengthening of pretensioned prestressed concrete beams having ruptured strands," *Journal of JSCE*, vol. 2, no. 1, pp. 25–38, 2014.

[9] L. A. Bisby, *Fire Behavior of FRP Reinforced or Confined Concrete*, Queen's University, Kingston, Ontario, Canada, 2003.

[10] JSJ 55, *Specification for Mix Proportion Design of Ordinary Concrete*, China Architecture and Industry Press, Beijing, China, 2002, in Chinese.

[11] GB50367, *Code for Design of Strengthening Concrete Structure*, China Architecture and Industry Press, Beijing, China, 2013, in Chinese.

[12] Y.-Z. Wu, H.-L. Lv, S.-C. Zhou, and Z.-N. Fang, "Degradation model of bond performance between deteriorated concrete and corroded deformed steel bars," *Construction and Building Materials*, vol. 119, pp. 89–95, 2016.

[13] H.-S. Lee, T. Noguchi, and F. Tomosawa, "Evaluation of the bond properties between concrete and reinforcement as a function of the degree of reinforcement corrosion," *Cement and Concrete Research*, vol. 32, no. 8, pp. 1313–1318, 2002.

[14] C.-H. Huang, "Effects of rust and scale of reinforcing bars on the bond performance of reinforcement concrete," *Journal of Materials in Civil Engineering*, vol. 26, no. 4, pp. 576–581, 2014.

[15] G. Mancini and F. Tondolo, "Effect of bond degradation due to corrosion—literature survey," *Structural Concrete*, vol. 15, no. 3, pp. 408–418, 2013.

[16] L. Chernin and D. V. Val, "Prediction of corrosion-induced cover cracking in reinforced concrete structures," *Construction and Building Materials*, vol. 25, no. 4, pp. 1854–1869, 2011.

[17] S. Coccia, S. Imperatore, and Z. Rinaldi, "Influence of corrosion on the bond strength of steel rebars in concrete," *Materials and Structures*, vol. 49, no. 1-2, pp. 537–551, 2016.
[18] R. Tepfers, "Cracking of concrete cover along anchored deformed reinforcing bars," *Magazine of Concrete Research*, vol. 31, no. 106, pp. 3–12, 1979.
[19] S. Pillay, U. K. Vaidya, and G. M. Janowski, "Effects of moisture and UV exposure on liquid molded carbon fabric reinforced nylon 6 composite laminates," *Composites Science and Technology*, vol. 69, no. 6, pp. 839–846, 2009.
[20] X. Cheng, Y. Baig, and Z. Li, "Effects of hygrothermal environmental conditions on compressive strength of CFRP stitched laminates," *Journal of Reinforced Plastics & Composites*, vol. 30, no. 2, pp. 110–122, 2011.
[21] A. Krishnan and C. Oskay, "Modeling compression-after-impact response of polymer matrix composites subjected to seawater aging," *Journal of Composite Materials*, vol. 46, no. 22, pp. 2851–2861, 2012.